Appl Compos Mater (2012) 19:97–115
DOI 10.1007/s10443-010-9184-5

Static and Fatigue Behaviour of Hexagonal Honeycomb Cores under In-plane Shear Loads

Gabriel Bianchi · Guglielmo S. Aglietti · Guy Richardson

Received: 12 October 2010 / Accepted: 19 December 2010 / Published online: 13 January 2011

Abstract Due to their high specific strength and high specific stiffness properties the use of honeycomb panels is particularly attractive in spacecraft structures. However, the harsh environment produced during the launch of a satellite can subject the honeycomb cores of these sandwich structures to severe quasi-static and dynamic loads, potentially leading to static or early fatigue failures. Knowledge of the static and fatigue behavior of these honeycomb cores is thus a key requirement when considering their use in spacecraft structural applications. This paper presents the findings of an experimental test campaign carried out to investigate the static and fatigue behaviors of aluminum hexagonal honeycomb cores subject to in-plane shear loads. The investigation involved carrying out both static and fatigue tests using the single block shear test method. These results are also discussed in relation to the observed damage and failure modes which have been reported for the statically tested specimens and for the fatigue tested specimens at various stages of fatigue life. As well as conducting tests for the more conventional principal cell orientations (L and W), results are also presented for tests carried out at intermediate orientations to investigate the variation of core shear strength with loading orientation. The results are further investigated using explicit non-linear finite element analysis to model the buckling failure mechanisms of the tested cores.

Keywords Honeycomb core · Shear strength · Fatigue · Buckling · Nonlinear finite element analysis

Nomenclature

G	Shear modulus
P	Load
b	Width of coupon

G. Bianchi (✉) · G. S. Aglietti
University of Southampton, Southampton, Hampshire SO17 1BJ, UK
e-mail: g.bianchi@soton.ac.uk

G. Richardson
Surrey Satellite Technology Limited, Guildford, Surrey GU2 7YE, UK

l	Length of coupon
t	Thickness of core
τ	Shear stress
$\Delta P/\Delta u$	Slope of load displacement curve

1 Introduction

Honeycomb sandwich construction is increasingly being used in the aerospace industry as a reliable and cost effective way of producing high strength, lightweight flight vehicle structures. Amongst the many types of sandwich structures developed to date, honeycomb panels are one of the best known. Honeycomb panels are advanced sandwich elements consisting of low modulus lightweight cellular (honeycomb) core sandwiched between high modulus, high strength face sheets. The assembly maximizes stiffness-to-weight ratio and bending strength-to-weight ratio, resulting in a panel structure that is particularly effective at carrying both in-plane and out-of-plane loads. Other advantages offered by honeycomb sandwich construction include low thermal conductivity and good sound insulating capacity.

Despite these attributes, as for other advanced composites, the application of honeycomb sandwich panels in primary aircraft and spacecraft structures has been limited in the past by the poor knowledge of their behavior under complex dynamic loads. In fact, even though these sandwich composites have been studied since they were first developed a large research effort is still ongoing in order to gain a better understanding of their static and fatigue behavior and make their use more widespread and attractive in more demanding structural applications.

At Surrey Satellite Technology Limited (SSTL) aluminum honeycomb sandwich panels are often used in the primary structures of the spacecrafts they develop. The development of a satellite represents a great investment so when considering the use of honeycomb panels a good knowledge of their strength, durability and damage tolerance is of paramount concern. The performance of a honeycomb panel is largely defined by its core type. Apart from maintaining a separation between the two face sheets and thus strengthen the bending stiffness of the panel, the honeycomb core also has the role carrying out-of-plane shear stresses.

Noteworthy studies on the mechanical properties of honeycomb cores have been conducted by other investigators in the past. Gibson and Ashby [1] studied the in-plane stiffness of honeycomb cores according to the bending model of cell edges. Masters and Evans [2] developed a theoretical model for predicting the in-plane elastic stiffness of honeycomb cores based on the deformation of honeycomb cells. Becker [3] studied the effective in-plane stiffness of honeycomb cores and the thickness effect using the closed form description. The determination of the out-of-plane shear properties of honeycomb cores is more challenging. The exact calculation of the shear modulus can only be done numerically. By making some simplifying assumptions Kelsey et al [4]. developed a series of theoretical expressions to determine the lower and upper bounds of the two shear moduli of honeycomb cores. Grediac [5] used the finite element method to calculate the transverse shear modulus as well as the state of stress in the honeycomb walls. Mereghni et al. [6] presented a new analytical method to analyze the out-of-plane stiffness of honeycomb cores based on the modified laminate theory. To present date, few studies have been conducted on the shear strength and shear failure modes of honeycomb cores. In Heimbs [7] a virtual testing technique using dynamic finite element simulation is proposed as an alternative to costly prototype testing when considering new sandwich core designs. The technique was

developed to predict both the mechanical behavior and the failure mechanism and a comparison of numerical and experimental results is presented for Nomex honeycomb core and two types of foldcore. Lee et al. [8]. investigated the compressive and shear deformation behavior and failure mechanism of sandwich composites consisting of Nomex honeycomb cores and 2024 aluminium alloy face sheets. Pan et al. [9]. experimentally investigated the shear deformation behavior and failure process of 5056 aluminum alloy honeycomb cores using the single block shear test and compared the results with a theoretical model based on shear strength formulas for thin plates. However, the experimental shear strength results obtained were significantly higher than the theoretical ones. This highlights the need for further investigations in this area. Furthermore, apart from an early work from the present authors [10], there are no works which consider the behavior of honeycomb cores under in-plane shear dynamic loads. The variation of static core shear strength and shear modulus is another area which has not been investigated in the literature. These areas represent the focus of the work presented here which is based on an extensive test campaign carried out to investigate the shear behavior of aluminum alloy hexagonal honeycomb cores under both static and cyclic loads. The test campaign involved conducting both static and fatigue single block shear tests in accordance with ASTM standards C273 and C394 [11, 12] respectively. The results obtained from the static tests were further investigated using the finite element method to model the failure modes.

2 Material Specimens

Two types of specimens incorporating two types of aluminum hexagonal cores with designations 5/32-5056-0.0015 and 1/8-5056-0.002 were tested under both static and fatigue loads (see Table 1). These cores have densities of 5.3 lb/ft^3 (85 kg/m^3) and 8.1 lb/ft^3 (130 kg/m^3) respectively and cell size of 4 mm and 3.2 mm respectively. For conciseness the two core types will be referred to using their density in lb/ft^3 in the rest of this paper. Both cores are produced in a conventional manner by expanding stacks of ribbon foils which were bonded to each other at regular intervals. This process produces cell walls with double thickness along the ribbon direction where the bonds are located. It is usual to refer to the ribbon direction and the expansion directions as the longitudinal (L) and transverse (W) directions respectively. Owing to the double thickness of the ribbon orientated cell walls the honeycomb core has significantly higher stiffness and shear strength in the L direction.

Although the main focus of the investigation is the honeycomb core, the test coupons incorporated the entire sandwich structure which also included the face sheets. This was

Table 1 Quoted properties of tested cores [13]

Property	Core type	
	5/32-5056-0.0015	1/8-5056-0.002
Cell Size [mm]	4.0	3.2
Density [kg/m^3]	85	130
Shear Strength L [MPa]	3.66	6.20
Shear Modulus L [MPa]	586	986
Shear Strength W [MPa]	2.14	3.59
Shear Modulus W [MPa]	228	301

done to check the overall manufacturing quality and expose any anomalous failure modes—in particular adhesive failures between the core and the face sheets. The face sheets were bonded to the core using Redux 319 adhesive film. For both types of cores the coupons were 15 mm thick and incorporate 0.5 mm thick 2014 aluminium alloy face skins. Both the static and fatigue test coupons were sized in accordance to ASTM standard C273, and were 190 mm in length and 60 mm in width. The coupons were obtained by sectioning large panels to the specified dimensions. By appropriately sectioning the panels, coupons (for both core types) were made for the principal orientations L and W (with the ribbon walls aligned parallel and normal to the longitudinal axis of the coupon respectfully). These are the orientations that are normally looked at when investigating the shear properties of hexagonal honeycomb cores; however, to investigate the variation of core behavior with loading orientation coupons were also made with cell orientations at angles other than 0° or 90° to the longitudinal axis of the coupon. Table 2 details the cell orientations that were investigated in the static and fatigue tests that were carried out.

3 Experimental Method

Both static and fatigue tests were conducted through the shear test fixture shown in Fig. 1. The force is transmitted to the coupon through bonded loading plates that are subject to opposing tensile or compressive displacements which result in a shear force on the sandwich core. In order to maintain self alignment and to eliminate bending moments two universal joints are used at both ends of the test fixture. In accordance to ASTM standard C273 the plate length and the distance between the universal joints is such that the line of action of the load passes through the diagonally opposite corners of the sandwich. The test does not produce pure shear stress, but the coupon length is prescribed so that secondary stresses have a minimum effect.

All the tests were conducted on an Instron 8802 universal servo-hydraulic testing machine controlled by an Instron electronic unit. The machine is equipped with a 100 kN load cell and an LVDT incorporated in the cross-head to measure the stroke. The load and cross-head displacement signals were recorded through an external PC using a data acquisition system. For the static tests the relative motion between the bonding plates was accurately measured using a strain gage extensometer (see Fig. 2).

4 Static Test Results

As discussed in Section 2 static tensile tests for 5.3 and 8.1 cored coupons were conducted for various cell orientations. All the tests were carried out at room temperature (~22°C) in displacement control at a cross-head speed of 0.5 mm/min. Failure load was taken as the

Table 2 Tested core orientations

Core type	Orientations	
	Static	Fatigue
5/32-5056-0.0015	0° (L), 45°, 90° (W)	0° (L), 45°, 90° (W)
1/8-5056-0.002	0° (L), 22.5°, 45°, 77.5°, 90° (W)	90° (W)

Fig. 1 Image of test fixture in operation

Fig. 2 Strain gage extensometer applied to bonding plates

peak of the load vs. displacement curves. The corresponding values of shear stress were found using the following expression

$$\tau = \frac{P}{l^{*}b} \tag{1}$$

where τ is the shear stress, P is the load applied to the coupon, l is the length of the coupon, and b is the width of the coupon. As the relative movement of the bonding plates was directly and accurately measured using an extensometer, from the obtained curve slopes, it was also possible to calculate the shear moduli. This was done using the following expression

$$G = \frac{(\Delta P/\Delta u)t}{l^{*}b} \tag{2}$$

where G is the shear modulus, $\Delta P/\Delta u$ is the slope of the load–displacement curve and t is the thickness of the core.

4.1 Principal Orientations Tests

Even though the 5.3 and 8.1 cores are standard aerospace grade cores and values for their shear modulus and ultimate strength for the principal L and W orientations can be found in reference manuals or standards (e.g. European Space Agency (ESA) Composite Design Handbook [13]), static testing was carried out in these orientations to see how closely the cores matched the quoted values. The load vs. crosshead displacement curves obtained from the tests are shown in Fig. 3. As expected, for both core types, the maximum achieved loads are significantly greater for the L oriented coupons than for the W oriented coupons. From the graph it can also be seen that, owing to its higher density, the 8.1 core has significantly greater shear strength than the 5.3 core. For all the tests failure occurred in the honeycomb cores of the coupons which plastically deformed due to shear buckling of the cell walls (see Fig. 4). In Fig. 3 no significant difference in slope can be seen in the linear regions of the curves indicating that the stiffness of the cores cannot be captured from the crosshead displacement data. This is because at crosshead level the displacement of the large test fixture is also being measured. In order to also obtain stiffness data from the coupons the relative movement

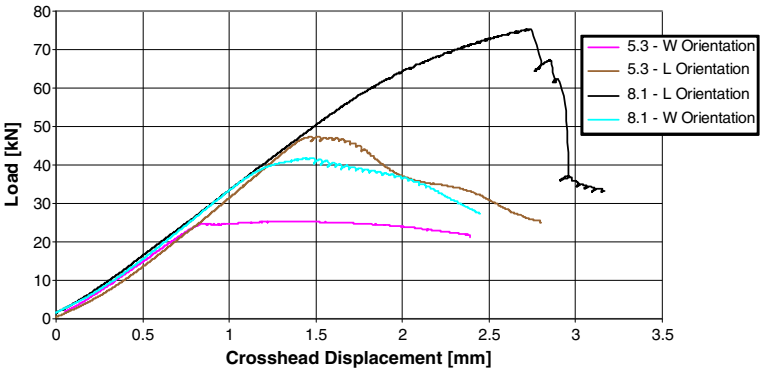

Fig. 3 Load versus cross-head displacement curves obtained by testing the two core types in the principal orientations

(a) L Orientation

(b) W Orientation

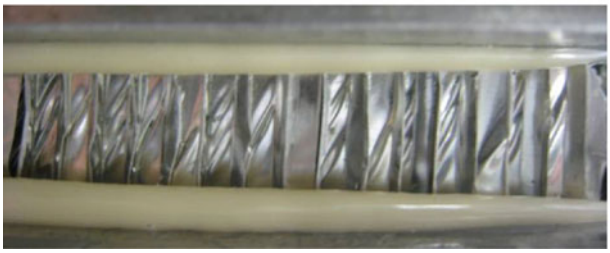

(c) 45 Orientation

Fig. 4 Failure mode of core in L, W and 45 orientations

between the bonding plates was directly measured using an extensometer. Curves based on extensometer data from these tests are presented in the next section together with curves obtained from testing in other orientations.

Using Eq. 1 it was possible to obtain the shear stress values corresponding to the load maximums obtained from the tests. From the extensometer data and using Eq. 2 it was possible to obtain the shear modulus values. The calculated shear strength and shear modulus results are summarized in Table 3 where they are also compared with the quoted typical values from the ESA Composite Design Handbook [13]. The shear strength results are all slightly higher but compare relatively well with the quoted values with the highest difference of the order of just 10% for the 5.3 core in the L orientation. The shear modulus results also compare very well with the quoted values for both the 5.3 and the 8.1 core. Overall then the tests confirm that the cores tested display the mechanical properties expected for their specifications. As the quoted values were obtained using the ASTM standard method, the results also confirm that the test method conforms to ASTM C273 and that fixturing system was working correctly.

Table 3 Results obtained by testing in the principal orientations and comparison with quoted values from the ESA Manual [13]

	5.3 Core				8.1 Core			
	Strength [MPa]		Modulus [MPa]		Strength [MPa]		Modulus [MPa]	
	L	W	L	W	L	W	L	W
Experimental results	4.16	2.18	586.0	228.0	6.61	3.60	1036.6	343.8
Quoted typical values	3.65	2.14	576.5	245.2	6.21	3.59	986.0	352.0

4.2 Angled Orientations Tests

From Table 3 it can be seen that for both core types the variation in mechanical shear properties from the L orientation to the W orientation is significant. To investigate how these properties transition from the L orientation to the W orientation a series of tests were conducted on coupons with cells oriented at various angles to the longitudinal axis of the coupon (see Table 2). The orientations tested were limited by the number of coupons that could be obtained from the available panel specimens. For the 5.3 core, the 45 deg orientation was tested in addition to the principal orientations. Figure 5 shows the obtained load vs extensometer displacement curves for the 45 deg orientation and the principal orientations plotted together. From the graph it can be seen that using the extensometer measurement it is possible to capture the stiffness variation between the different core orientations. For the 45 deg orientation it would be reasonable to expect a mechanical behavior somewhere between the L orientation and the W orientation, but from this graph it can be clearly seen that, although the stiffness of the core increases, its strength does not when going from the W orientation to the 45 deg orientation; on the contrary it decreases slightly (this is also confirmed from the results obtained from the fatigue tests presented in Section 5). As can be seen from Table 2 for the 8.1 core more orientations were tested. The load vs extensometer displacement curves obtained for these tests are shown in Fig. 6. For

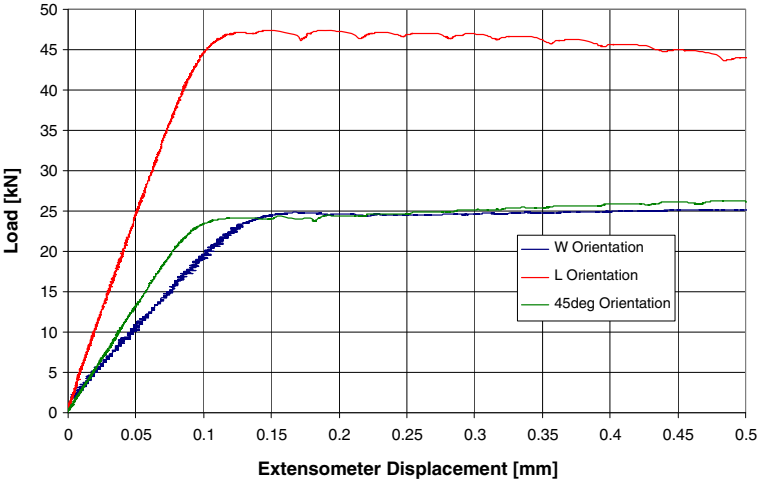

Fig. 5 Load vs extensometer displacement curves obtained for the 5.3 core

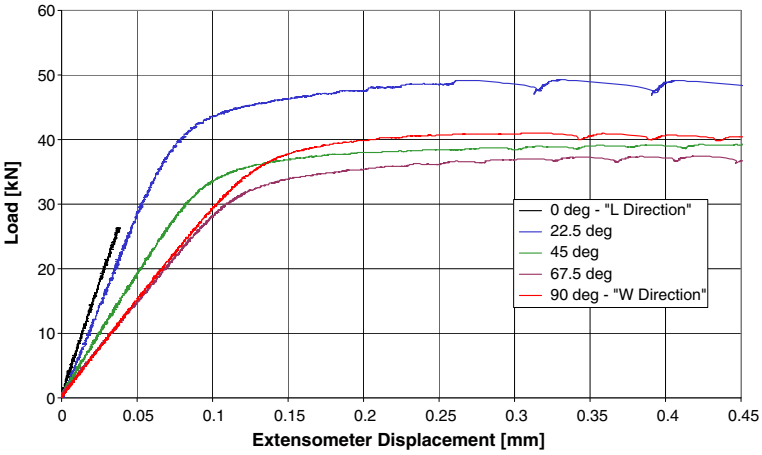

Fig. 6 Load vs extensometer displacement curves obtained for the 8.1 core

the L orientation test the extensometer was only used for the initial part of the test to obtain the shear modulus of the core and was then removed to prevent the possibility of damaging the extensometer as a result of coupon/loading panel debonding (hence way the curve shown for this test is truncated). This could have happened since in the L orientation the shear strength of the 8.1 core is close to the maximum strength that can be achieved from the adhesive used to bond the coupons to the loading plates. However, for this test no adhesive failure occurred and the coupon failed in the core as intended (the full load vs crosshead displacement curve can be seen in Fig. 3). From Fig. 6 it can be seen that, as for the 5.3 core, while the shear modulus increases slightly the shear strength does not when going from the W orientation to the 45 deg orientation. On the contrary there is a slight decrease in shear strength and looking at the 67.5 deg orientation there is even a greater decrease. This can be clearly seen in Fig. 7 where the maximum shear strength results obtained from the tests are plotted against cell orientation. From this graph it can be seen that for both core types the shear strength only increases significantly when the loading orientation decreases below 45 deg, below which as loading orientation decreases the strength increase rate grows until the maximum strength is reached at 0 deg (i.e. the L

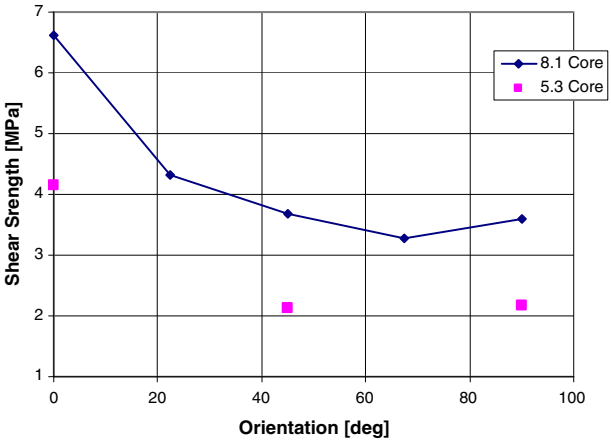

Fig. 7 Variation of measured shear strength with cell orientation for the 8.1 core

orientation). A similar behavior can be seen in Fig. 8 for the shear modulus variation with loading orientation.

5 Fatigue Test Results

The objective of the fatigue tests was to obtain basic knowledge of the fatigue behavior of the tested honeycomb cores by producing S-N diagrams and observing the failure modes. For the 5.3 core tests were conducted for the L, W and 45° orientations. For the 8.1 core, tests were carried out only for the W orientation. Tests for the L orientation were not carried out since it was not possible to guarantee a strong enough bond between the specimen and the loading plates (due to the high strength of the specimen itself in this orientation). All tests were conducted at room temperature in load control at load amplitude values chosen on the basis of the static test results. For all the tests the applied load was sinusoidal with a ratio $R=-1$ (i.e. fully reversed). The fully reversed load profile subjects the coupon to alternating tensile and compressive stresses and was chosen because it induces the highest fatigue damage and hence is representative of the most severe loading scenarios. The fatigue life of the coupons is characterized in terms of the number of cycles to ultimate failure. For all the tested coupons failure was in the core and no core/face sheet debonding occurred.

The S-N fatigue curves obtained for the 5.3 core in both the L and the W orientations are both shown in Fig. 9. As expected the lifetime of the core is significantly longer in the L configuration than in the W configuration for equivalent values of stress amplitude. However, from the trendlines, it is possible to see that as stress amplitude reduces the lifetime increases slightly more rapidly for the W orientation. Plotting these fatigue curves in terms of normalized load level (expressed as percentage of static ultimate load) versus displacement (see Fig. 10) it is possible to see that, for load levels above ~20%, the achieved lifetime for the W configuration is actually higher than for the L configuration. This indicates that even though the core is significantly stronger in the L direction it seems to be (in relative terms) more effective at resisting fatigue damage in W direction.

From visual inspection of the free sides of the failed coupons a difference was noticed in the failure modes experienced at different load levels. At high load levels both coupon types fail in a very similar way to the coupons that were subjected to the static tests, with the core plastically deforming as the cell walls buckle under shear, but no visible cracks

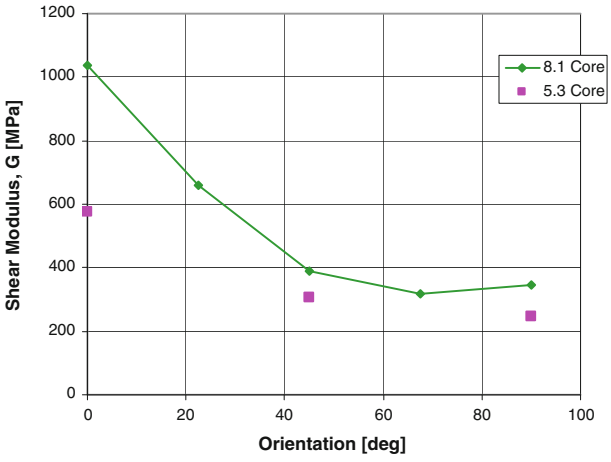

Fig. 8 Variation of measured shear modulus with cell orientation for the 8.1 core

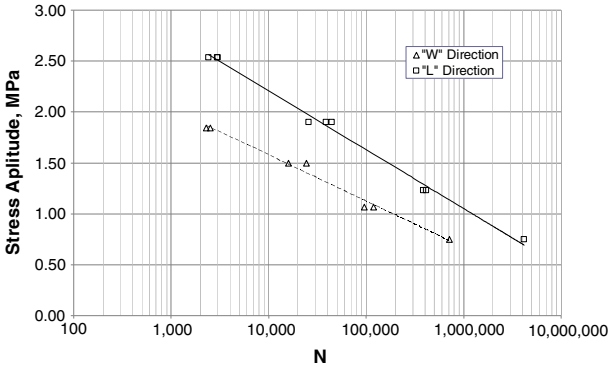

Fig. 9 S-N curve for tested 5.3 cored coupons in L and W directions

appearing. For lower load levels the development of cracks was observed during the lifetime of both the L and W configuration samples (see Figs. 11 and 12). However, it was also noticed that crack development is different for the two cell orientations.

For the L configuration cracks appear to initiate at the face sheets and propagate diagonally towards the centre as the test progresses (see Fig. 11), while for the W orientation cracks initiate on the inclined single thickness cell walls at cell wall boundaries and develop diagonally to the next boundary (see Fig. 12). For equivalent load levels the cracks develop to a significantly greater length in the L orientation than in the W orientation. This is because in the W orientation the cell wall boundaries also act as crack boundaries since each diagonal cell wall is connected to one half of a double cell wall which is aligned at 90° to the loading axis. On the contrary in the L orientation none of the cell walls are at 90° with the loading axis and consequently all the cell walls are subject to shear stresses and cracks are allowed to grow along each ribbon from cell wall to cell wall. These differences in crack propagation are likely to have a significant effect on the fatigue life of the specimens and offer a good explanation as to why the core is more effective at resisting fatigue damage in the W direction; particularly for lower stress amplitudes (i.e. high cycle fatigue) where cracks have to reach a large critical length before failure occurs.

For the 5.3 core fatigue tests were also carried out for the 45 deg orientation. The S-N curve obtained from these tests is shown in Fig. 13 where it is also compared with the curves obtained for the L and W orientations. From the S-N diagram it can be clearly seen that the lifetime of the coupon is slightly lower in the 45 deg orientation compared to the W

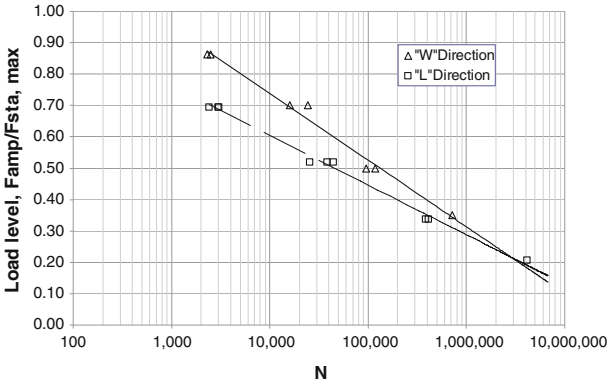

Fig. 10 Load level versus cycle no. curves for tested 5.3 cored coupons in L and W directions

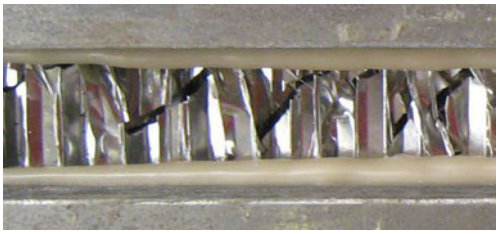

Fig. 11 Crack development in core after fatigue testing in L direction at 34% of the static ultimate load ~400000 cycles

orientation for equivalent load levels. This is in agreement with the slightly lower static strength that was obtained from static testing.

Figure 14 shows the fatigue curve obtained for the 8.1 core in the W orientation compared with the one obtained for the 5.3 core in the W direction. From the graph it can be seen that the lifetime of the 8.1 core is significantly higher owing to its higher static strength.

The displacement amplitude of the crosshead was also recorded during the fatigue tests to see how the stiffness varied during the lifetime of the specimens. From this data it was found that there is very little variation in displacement amplitude and consequently of the sample stiffness during most of the fatigue lifetime. Any significant changes in displacement amplitude were very quickly followed by coupon failure. This suggests that stiffness is probably not an effective monitoring measure for the health of honeycomb cores subject to shear loads.

6 Finite Element Modeling

6.1 Model Description

To further study the effect of loading orientation on the shear strength of the tested honeycomb cores an investigation using the finite element method was also carried out. In order to reduce the requirement on computational resources instead of modeling the whole coupon, the approach taken here was just to consider a representative cell and apply appropriate boundary conditions. To simulate the buckling failure mechanism of the cell walls Nastran's Implicit Nonlinear solution (SOL 600) code was used to process the model. The cell models were meshed using 4-node quadrilateral shell elements and constructed based on the geometrical dimensions of the 8.1 and 5.3 core cells.

The cell model is constrained at the base in the x, y and z global coordinate directions and loaded by applying a fixed displacement at the top in the desired direction. The loading

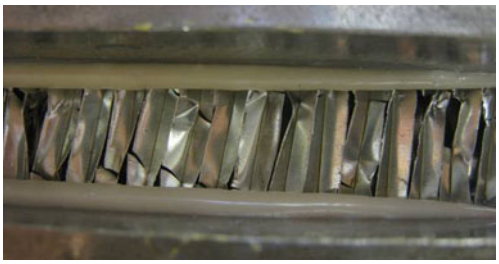

Fig. 12 Crack development in core after fatigue testing in W direction at 35% of the static ultimate load ~718394 cycles

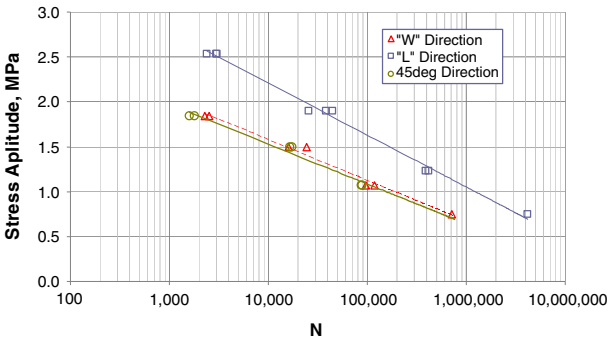

Fig. 13 Load S-N curve for tested 5.3 cored coupons in L, W and 45 deg directions

displacement is applied to a single node rigidly connected to the top edges of the cell walls via a multi point constraint (MPC). To avoid bending moments the cell is also constrained in the z global coordinate direction along its outer edges (see Fig. 15). To ensure in-plane loading and to avoid twisting all rotations are constrained for the loading node at the centre of the MPC. To obtain a displacement perfectly aligned with the specified displacement direction a constraint should be applied normal to it (a cross-axis constraint). If a cross-axis constraint is not applied the cell is allowed to drift sideways with respect to the displacement direction. When the displacement is applied in the principal orientations there is no significant tendency for the sideways drift. However, due to structural imbalance, this is not the case for the in between orientations for which the application of a cross-axis constraint has a significant effect on the obtained shear modulus and shear strength. In reality, in most cases, what happens is somewhere between having a fixed cross-axis constraint and fully free cross-axis displacements. This "in-between" condition can be simulated by using a spring element aligned to the cross-axis direction. In a real application the stiffness of the spring would depend on how the honeycomb panel is constrained and connected to its surrounding structural components. For the experimental case considered here the loading fixture has a tendency to maintain its original alignment and resists cross-axis displacements to a certain extent.

6.2 Modeling of Imperfections

Buckling instability is a notoriously challenging phenomenon to model using the finite element method and generally yields non-conservative over-estimations of the mechanical properties. The main reason for this is that normally the inherent

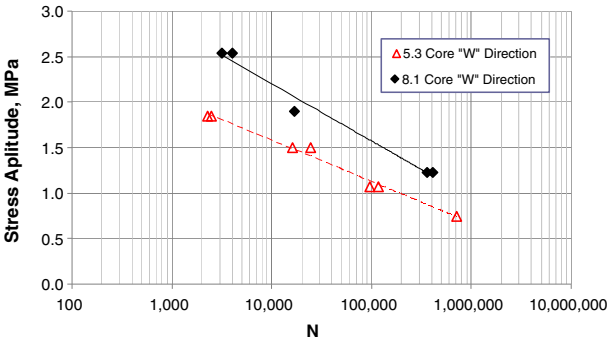

Fig. 14 Load level versus cycle no. curves for tested 8.1 and 5.3 cores in the W directions

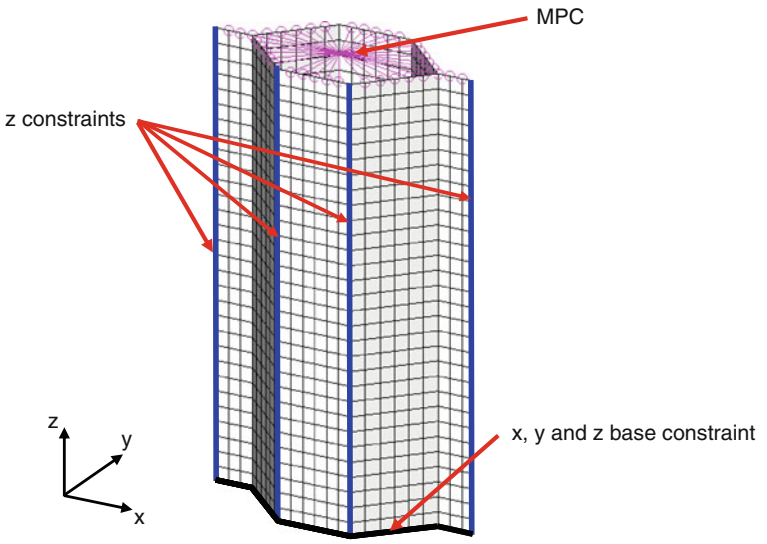

Fig. 15 Unit cell model with global coordinate system and boundary conditions

imperfections of a real structure are not modeled. These imperfections are particularly pronounced for the cellular structures considered here. The expansion process can only be controlled to a certain extent and a perfect hexagonal geometry is not achievable. Likely imperfections include [14]: uneven cell walls, irregular cell geometry, cell wall intersections with rounded rather than perfect angular corners, and non constant wall

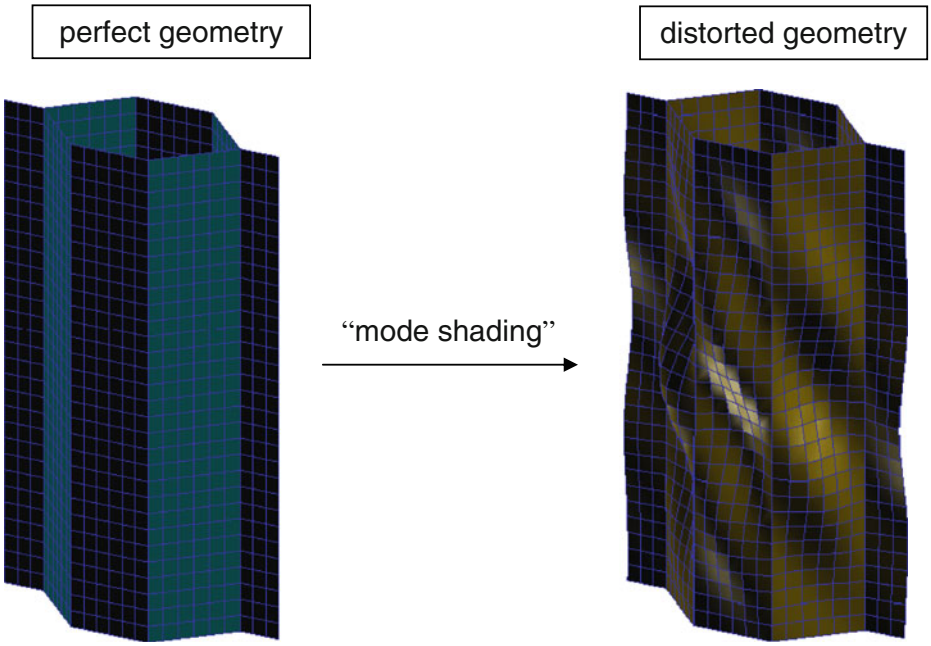

Fig. 16 Introduction of geometrical imperfection via mode shading (distortion exaggerated for illustration)

thickness. There are several ways to account for effect of such imperfections in a finite element model.

One method is to introduce imperfections in the mesh. An effective way of doing this is via "mode shading", whereby the nodes' coordinates are modified based on the eigenvalues obtained by running an eigenvalue buckling analysis (see Fig. 16). The degree of imperfection can be scaled as a percentage of nominal wall thickness (typically between 5 and 30%).

Another way of accounting for imperfections is to vary the thickness properties of the shells across the mesh (whilst keeping the overall average equal to the nominal thickness). A further alternative is to reduce the overall cell properties (material properties and wall thickness) for the whole model. This is also justifiable since in reality the weakest or thinnest regions of the core are going to drive the failure strength of the core [15].

In order to appropriately account for imperfections the best approach is to apply more than one of the above techniques in conjunction. Here mode shading and thickness variation were used to obtain more realistic results. The magnitudes of the imperfections were applied based on manufacturing tolerance estimates and then adjusted to reduce the over-estimation in predicted failure load compared with the experimental data. However, a perfect correlation was not sough since the main aim of the study was to investigate the effect of loading orientation and see if the same trends observed from the experiments would be obtained. For each cell model the same imperfection parameters were used for all the load cases.

6.3 Results from Finite Element Analysis

Using an appropriate spring stiffness to account for the behavior of the loading fixture it was possible to obtain equivalent shear stress vs. relative displacement (between base and top of cell) curves as shown in Fig. 17 and Fig. 18 for the 5.3 core. Figure 17 only shows the directions which were also experimentally tested and the experimental curves are included for comparison. The deformed cell shapes obtained for these analysis runs are

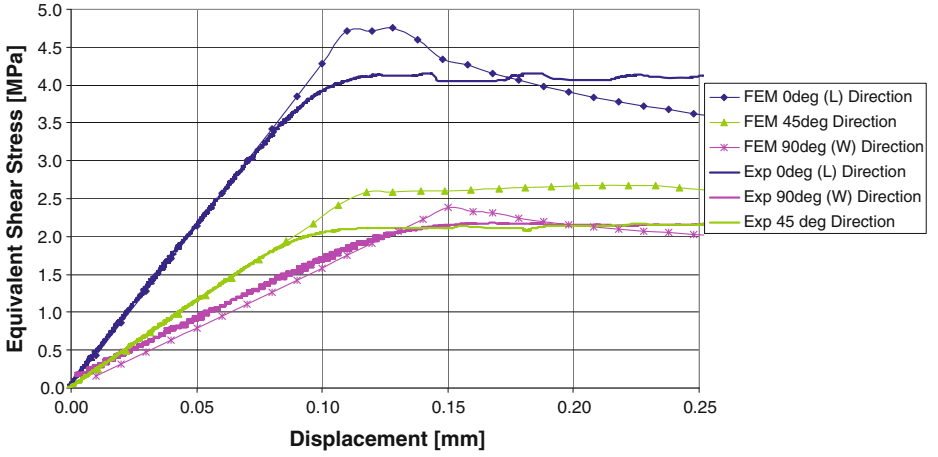

Fig. 17 Comparison between experimental and finite element model (FEM) equivalent shear stress vs. displacement curves

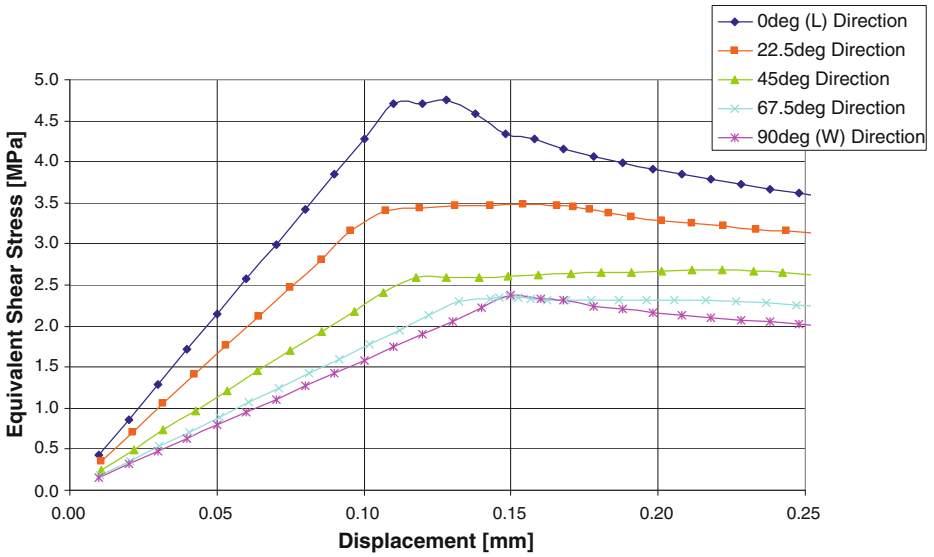

Fig. 18 Finite element model (FEM) equivalent shear stress vs. displacement curves for all the directions considered

shown Fig. 19. From these curves it can be seen that the stiffness is matched very well for all the considered directions; however, the failure loads are over predicted. This is to be expected for the reasons described above. The over prediction tendency is slightly higher for the 0 deg L direction were failure is dominated by buckling to a greater extent. Figure 18 shows the FEM curves from all the loading directions modeled. From these curves the predicted variation of shear strength with loading direction for the 5.3 core is plotted as shown in Fig. 20 where it is also compared with the experimental values. An

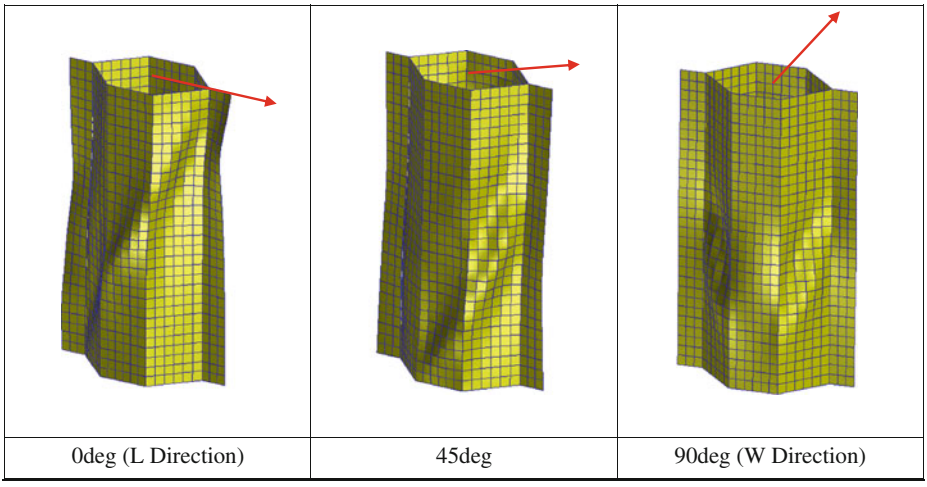

Fig. 19 Cell deformations obtained from simulations runs loading the model in different directions (shear strain is ~2% for all cases)

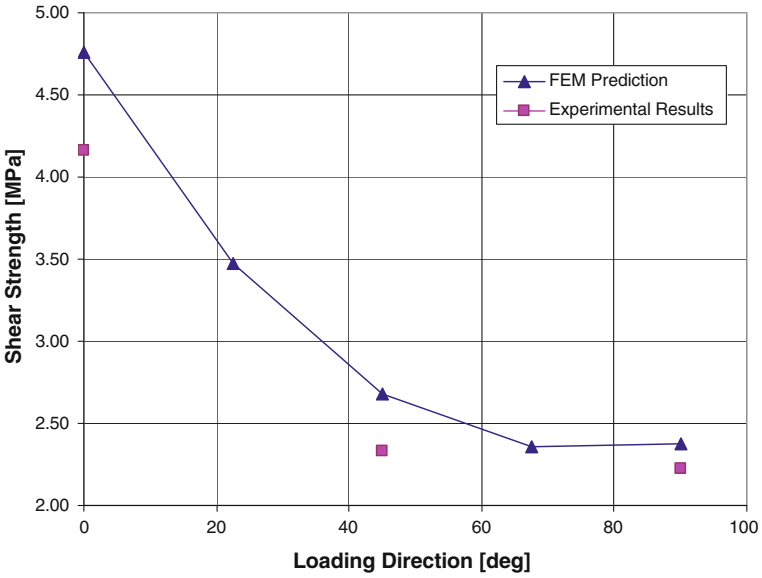

Fig. 20 Variation of shear strength with loading direction for the 5.3 core

analogous graph was also obtained by modeling the 8.1 core (see Fig. 21). Despite the over prediction it can be seen that for both core types the predicted variation trend is in agreement with the experimental results (seen for both core types) which suggest that the shear strength of the core only starts to increase significantly when the loading angle direction decreases below 45 deg.

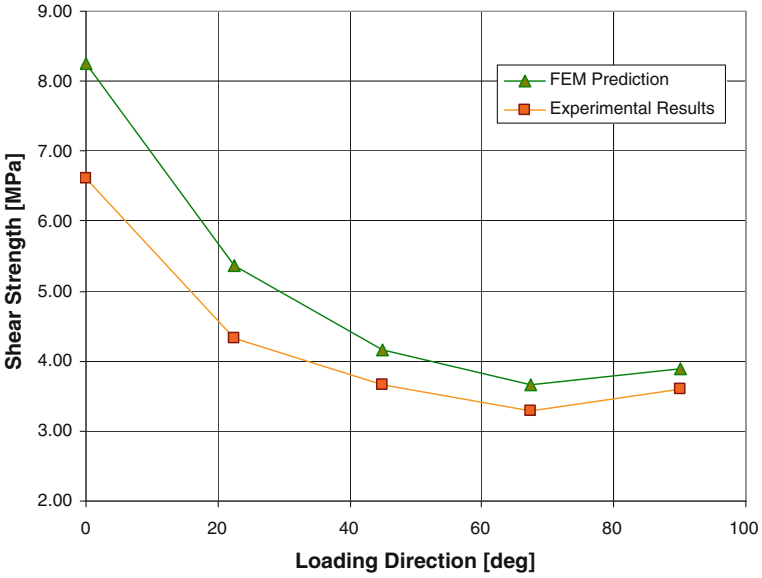

Fig. 21 Variation of shear strength with loading direction for the 8.1 core

7 Conclusions

Static and fatigue shear block tests were carried out on both 5.3 and 8.1 cored coupons in various orientations. For the static tests conducted in the principal orientations the results were found to be in agreement with the typical quoted values of both core types. Data relevant to tests carried out at angles other than the principal orientations is not available in reference manuals and no studies are reported in the literature. From the tests carried out here it was found that for both core types the shear strength and the shear modulus had a non-linear relationship with loading orientation. Contrary to what is normally assumed, it was also found that (all be it by a small margin) the W orientation was not the weakest orientation. For both core types it was found that the shear strength only increases significantly when the loading orientation is decreased below 45 deg below which the increase rate grows until the maximum strength is reached at 0 deg (i.e. the L orientation).

Using the finite element method it was determined that this non-linear relationship is due to the tendency of the core to also displace cross-axis with respect to the loading orientation when the load is not applied parallel to one of the principal orientations. Constraining this cross-axis displacement has a significant effect on the relationship of both the shear modulus and the shear strength of the core with loading orientation. In real applications the level of cross-axis constraint will vary from case to case depending on how the panel is connected to surrounding structural components. Fully constraining the cross-axis displacement will give the highest core strength and core modulus values (for a given loading orientation) and a near linear relationship with loading orientation. On the other hand a free cross-axis constraint gives the lowest values of core strength and modulus with a minimum value of shear strength potentially sensibly lower than for the W orientation.

As expected, from the fatigue tests it was found that for equivalent stress amplitudes, the fatigue lifetime of the specimens was longer in the L direction compared to the W direction. This is because the core has a significantly higher static ultimate strength in the L direction; however, in terms of load level (i.e. percentage of static ultimate strength) versus lifetime it was found that the core is actually more effective at resisting fatigue damage in the W orientation. By visual inspection of the failed specimens it was found that this may be attributed to the fact that crack propagation appears to be significantly inhibited by cell wall boundaries in the W orientation. For the 5.3 core fatigue tests were also conducted for the 45 deg orientation. From the S-N curve obtained from these tests it was observed that the lifetime of the coupon in this orientation was slightly lower compared to the W orientation.

References

1. Gibson, L.J., Ashby, M.F.: Cellular Solids: Structure and Properties, 2nd edn. Cambridge University Press, Cambridge (1997)
2. Masters, I.G., Evans, K.E.: Models for the elastic deformation of honeycombs. Compos Struct **35**, 403–22 (1996)
3. Becker, W.: Closed-form analysis of the thickness effect of regular honeycomb core material. Compos Struct **48**, 67–70 (2000)
4. Kelsey, S., Gallatly, R.A., Clark, B.W.: The shear modulus of foil honeycomb core. Aircr Eng **30**, 294–302 (1958)

5. Grediac, M.: A finite element study of the transverse shear in honeycomb cores. Int J Solids Struct **30** (13), 1777–88 (1993)
6. Meraghni, F., Desraumaux, F., Benzeggagh, M.L.: Mechanical behavior of cellular core for structural sandwich panels. Compos A **30**, 767–79 (1999)
7. Heimbs, S.: Virtual testing of sandwich core structures using dynamic finite element simulations. Comput Mater Sci **45**, 205–216 (2009)
8. Lee, H.S., Hong, S.H., Lee, J.R., Kim, Y.K.: Mechanical behavior and failure process during compressive and shear deformation of honeycomb composite at elevated temperatures. J Mater Sci **37**, 1265–72 (2002)
9. Pan, S.D., Wu, L.Z., Sun, Y.G., Zhou, Z.G., Qu, J.L.: Longitudinal shear strength and failure process of honeycomb cores. Compos Struct **72**, 24–46 (2006)
10. Bianchi G, Aglietti GS, Richardson G, "Experimental Investigation of Static and Fatigue Behaviour of Honeycomb Panels under In-plane Shear Loads". In: 50th AIAA/ASME/ASCE/AHS/ASC Structures, Structural Dynamics, and Materials Conference, Palm Springs, Ca, USA, 4–7 May 2009
11. ASTM C273, Standard test method for shear properties of sandwich core materials
12. ASTM C394, Standard test method for shear fatigue of sandwich core materials
13. Composite Design Handbook, European Space Agency, ESA PSS-03-203
14. Hohe, J., Becker, W.: Effective stress-strain relations for two-dimensional cellular sandwich cores: Homogenization, material models, and properties. Appl Mech Rev **55**, 61 (2002)
15. Heimbs, S., Middendorf, P., Kilchert, S., Johnson, A.F., Maier, M.: Experimental and numerical analysis of composite folded sandwich core structures under compression. Appl Compos Mater **14**, 363–377 (2007)